Resonance Raman Evidence for the Presence of Two Heme Pocket Conformations with Varied Activities in CO-Bound Bovine Soluble Guanylate Cyclase and Their Conversion

Zhengqiang Li,[‡,§] Biswajit Pal,[‡,||] Shigeo Takenaka, Shingo Tsuyama, and Teizo Kitagawa*

Okazaki Institute for Integrative Bioscience, National Institute of Natural Sciences, Myodaiji, Okazaki 444-8787, Japan

Received May 26, 2004; Revised Manuscript Received August 31, 2004

ABSTRACT: Resonance Raman (RR) spectra of soluble guanylate cyclase (sGC) reported by five independent research groups have been classified as two types: sGC_1 and sGC_2. Here we demonstrate that the RR spectra of sGC isolated from bovine lung contain only sGC_2 while both species are observed in the spectra of the CO-bound form (CO−sGC). The relative populations of the two forms were altered from an initial composition in which the CO−sGC_2 form predominated, with the Fe−CO (ν_{Fe-CO}) and C−O stretching modes (ν_{CO}) at 472 and 1985 cm^{-1}, respectively, to a composition dominated by the CO−sGC_1 form with ν_{Fe-CO} and ν_{CO} at 488 and 1969 cm^{-1}, respectively, following the addition of a xenobiotic, YC-1. Further addition of a substrate, GTP, completed the change. GDP and cGMP had a significantly weaker effect, while a substrate analogue, GTP-γ-S, had an effect similar to that of GTP. In contrast, ATP had a reverse effect, and suppressed the effects of YC-1 and GTP. In the presence of both YC-1 and GTP, vinyl vibrations of heme were significantly influenced. New CO isotope-sensitive bands were observed at 521, 488, 363, and 227 cm^{-1}. The 521 cm^{-1} band was assigned to the five-coordinate (5c) species from the model compound studies using ferrous iron protoporphyrin IX in CTAB micelles. Distinct from the 472 cm^{-1} species, both the 488 and 521 cm^{-1} species were apparently un-photodissociable when an ordinary Raman spinning cell was used, indicating rapid recombination of photodissociated CO. On the basis of these findings, binding of YC-1 to the heme pocket is proposed.

Soluble guanylate cyclase (sGC)[1] is a cytosolic heme-containing enzyme that catalyzes the conversion of GTP to cGMP, a primary messenger molecule in biological systems (*1*−*3*). This protein is a heterodimer ($\alpha\beta$) (*4*−*8*) containing a heme only in the β subunit (*9*, *10*) (coordinated to His105 in bovine lung sGC) (*11*). The enzyme controls smooth muscle relaxation (*12*), platelet aggregation (*13*), and neurotransmission (*14*), and serves as a physiological receptor for nitric oxide produced by an NO synthase. NO binds to the heme group, resulting in stimulation of catalytic activity by 200−400-fold (*15*, *16*).

Karlsson et al. (*17*) suggested that CO also activates sGC slightly, and indeed, 2−6-fold stimulation over basal activity by CO was confirmed by different groups (*6*−*8*, *14*, *18*, *19*). In the presence of a zenobiotic, YC-1, activation by CO is further increased to a level similar to that attained by NO alone (*19*). YC-1 inhibits platelet aggregation (*20*) and adhesion (*21*), and smooth muscle contraction (*22*). The compound serves as a novel inhibitor of phosphodiesterase with moderate potency and low enzyme specificity (*23*), and raises sGC activity by 6−12-fold (*24*). However, unexpectedly, YC-1 stimulates activity by 200−400-fold in the presence of CO (*19*, *24*). The mechanism of synergistic activation of sGC by CO and YC-1 remains to be elucidated.

The resting and activated states of sGC have been investigated spectroscopically with resonance Raman (RR) (*25*−*28*), MCD (*15*), EPR (*29*), and visible absorption spectroscopy (*15*, *16*, *30*). RR spectroscopy is a powerful tool for characterizing heme coordination environments, and several groups have independently examined RR spectra of sGC. Their results indicated two forms of sGC [tentatively designated sGC_1 and sGC_2 by Vogel et al. (*31*)]. Addition of heme to purified protein rendered sGC_1 NO-sensitive. The spectrum of the heme-incorporated protein appeared as a mixture of five-coordinate (5c) high-spin (HS) and six-coordinate (6c) low-spin (LS) species (*25*, *28*), and its CO adduct displayed an Fe−CO stretching (ν_{Fe-CO}) band at 492 cm^{-1}. In contrast, sGC_2 was isolated in the reduced form from bovine lung and entirely comprised 5c-HS (*26*, *27*). Its CO adduct gave the ν_{Fe-CO} band at 472 cm^{-1}. Addition of heme to the sGC_2 adduct had no effect, indicating an absence of free apoprotein in this preparation. The difference

* To whom correspondence should be addressed. E-mail: teizo@ims.ac.jp. Fax: +81-564-59-5229. Phone: +81−564−59−5225.

‡ These authors contributed equally to this work.

§ Present address: Key Laboratory for Molecular Enzymology and Engineering of the Ministry of Education, Jilin University, Changchun 130023, China.

|| Present address: Centre for Cellular and Molecular Biology, Uppal Road, Hyderabad 500 007, India.

[1] Abbreviations: sGC, soluble guanylate cyclase; GTP, guanosine 5′-triphosphate; cGMP, guanosine 3′,5′-cyclic monophosphate; SNP, sodium nitroprusside; PDE, phosphadiesterase; YC-1, 3-[5′-hydroxymethyl(2′-furyl)]-1-benzylindazole; CO−sGC, CO-bound form of sGC; NO−sGC, NO-bound form of sGC; ν_{Fe-CO}, Fe−CO stretching mode; ν_{CO}, C−O stretching mode; ν_{Fe-His}, Fe−His stretching mode; RR, resonance Raman; TEA, triethanolamine; DTT, 1,4-dithiothreitol; EDTA, ethylenediaminetetraacetic acid; β1(1−385), polypeptide of residues 1−385 of the β1 subunit of sGC; CO−β1(1−385), CO-bound form of β1(1−385); DMSO, dimethyl sulfoxide; SDS−PAGE, sodium dodecyl sulfate−polyacrylamide gel electrophoresis.

10.1021/bi0489208 CCC: $30.25
Published on Web 12/30/2004

in CO-related frequencies signifies appreciable variations in the polarity of heme pocket (*32*, *33*). The higher ν_{Fe-CO} frequency reflects a more polar environment when the trans ligand of CO is identical.

Recently, reports about the CO adduct of the heme-containing domain (β_{1-381}) of sGC expressed with *Escherichia coli* show that the ν_{Fe-CO} band appears at 474 cm^{-1} (sGC_1 type) and 492 cm^{-1} (sGC_2 type) in the absence and presence of YC-1, respectively (*34*, *35*). We demonstrate in this study that native sGC isolated from bovine lung initially contains only sGC_2 but its CO adduct comprises both types (with sGC_2 dominating), and exhibits complete and reversible conversion from sGC_2 to sGC_1 in the presence of YC-1 and GTP. However, this conversion is intermediate in the presence of YC-1 alone and negligible with GTP alone. Converted sGC contains a small quantity of 5c heme with CO as an axial ligand. ATP suppresses the synergistic effect of YC-1 and GTP, while GDP and cGMP have a significantly weaker effect.

MATERIALS AND METHODS

Purification of Soluble Guanylate Cyclase. The enzyme was purified from a fresh bovine lung by slight modification of the method of Tomita (*36*). Minced lung (4 kg) was homogenized into 4 L of buffer (25 mM TEA-HCl, 50 mM NaCl, 5 mM DTT, 1 mM EDTA, 1 mM benzamidine, and 1 mg/mL protease inhibitor) and centrifuged at 10000*g* for 20 min first. The supernatant was further centrifuged at 100000*g* for 30 min. Its supernatant was added to 1000 mL of DEAE-Sepharose Fast Flow (Amersham-Pharmacia Biotech) and stirred slowly with an overhead stirrer for 30 min. The unbound proteins were removed by vacuum filtration, and the remaining resin was washed twice with 1000 mL of homogenizing buffer. After the resin was resuspended in homogenizing buffer, the resin was packed to a 5 × 60 cm column and washed with homogenizing buffer for 4 h at 120 mL/h. The adsorbed sGC was eluted by 2 L of a NaCl solution at 120 mL/h with a linear gradient of NaCl (from 0.05 to 1.05 M), and the fractions containing NO-sensitive guanylate cyclase activity were collected. Ammonium sulfate was added to the collected fractions up to 23% saturation, and the resulting precipitate was removed by centrifugation at 15000*g* for 20 min. Ammonium sulfate was further added to the supernatant to 41% saturation. The precipitate was collected by centrifugation and suspended in a small volume of buffer A (25 mM TEA, 5 mM DTT, 1 mM benzamidine, and 1 mg/L protease inhibitor).

The suspension was dialyzed against buffer A overnight with three changes. After the addition of $MnCl_2$ to a final concentration of 4 mM, the dialysate was centrifuged at 15000*g* for 20 min and the supernatant run on a GTP−agarose column (100 mL) pre-equilibrated with buffer A containing 4 mM $MnCl_2$. The adsorbed column was washed with buffer A containing 4 mM $MnCl_2$ and eluted with buffer A having a linear gradient from 4 mM $MnCl_2$ to 8 mM ATP. The fractions containing NO-sensitive GC activity were concentrated using an Amicon-30 concentrator and dialyzed against buffer A. The dialysate was loaded onto a hydroxyapatite column (30 mL) pre-equilibrated with buffer A, and eluted with a linear gradient of phosphate (from 0 to 200 mM). The fractions containing NO-sensitive GC activity were concentrated with an Amicon-30 concentrator and further subjected to a gel filtration column (Superdex 200pg, Pharmacia) pre-equilibrated with 25 mM TEA-HCl (pH 7.4) containing 5 mM DTT. The fractions containing sGC were reconcentrated again with an Amicon-30 concentrator. Finally, glycerol was added to the concentrated sGC solution up to 20%, and the solution was frozen at 77 K.

Activity Assay. sGC activity was routinely measured as follows. The sample was incubated with 50 mM Tris-HCl (pH 7.4) containing 1 mM theophilline, 1 mM DTT, 1 mM GTP, and 1 mM Mg^{2+} at 37 °C for 5 min. After incubation, the reaction was terminated by rapidly cooling the mixture on ice. The amount of cGMP present in solution was measured using a [^{3}H]cGMP immunoassay system (Amersham, TRK 500). The effects of YC-1 on sGC activity were measured with the sGC solution containing 120 μM YC-1. YC-1 was dissolved in DMSO up to 10 mM and then was diluted to 5 mM with buffer containing 25 mM TEA and 5 mM DTT to avoid the formation of fine particles upon addition to the enzyme solution. For the assay of CO and CO/YC-1 activation of sGC, CO was incorporated into the assay solution with a gastight syringe. SNP was employed for measuring NO stimulation of sGC activity. The protein concentration was determined using the method of Bradford (*37*).

Gel Filtration. To examine the reversibility of YC-1 and GTP binding, YC-1- and GTP-bound CO−sGC were subjected to gel filtration following the measurement of absorption and RR spectra. Approximately 90 μL of the enzyme solution was centrifuged at 1000*g* and 4 °C for 30 min and then added to the Bio-Rad spin column (Bio-Spin30 Chromatography Column) pre-equilibrated with 25 mM TEA and 5 mM DTT. The eluted solution was brought into the Raman cell, and CO was incorporated, which was similar to the method used for the native protein.

Resonance Raman Spectroscopy. For Raman measurements, purified sGC was diluted to 12 μM (heme) using the formula ϵ_{mM}(heme) = 105 cm^{-1} at 432 nm, with 50 mM TEA buffer (pH 7.4) containing 5 mM DTT (and 20% glycerol in some cases). To obtain CO−sGC, ~60 μL of the solution was brought into an airtight Raman spinning cell. After the cell had been repeatedly degassed (to 0.1 mmHg) and filled with pure N_2 gas, CO was incorporated into the upper space of the Raman cell through a rubber septum using an airtight syringe. Raman scattering was excited with the 422 nm line of a diode laser (Hitachi Metal, ICD-430), the 413.1 nm line of a krypton laser (Spectra Physics, model 2016), or the 441.6 nm line of a He−Cd laser (Kinmon Electrics, KR1801C).

The scattered light at right angles was collected and dispersed with a single polychromator (Ritsu Oyokogaku, model MC-100DG), and detected using a liquid nitrogen-cooled charge-coupled device (CCD, Princeton Instruments, model LN/CCD-1300-PB). Raman shifts were calibrated with indene. The accuracy of frequencies is ±1 cm^{-1} for well-defined peaks. The sample temperature was kept at ~10 °C by flushing with cold N_2 gas. The laser power was generally 10 mW at the sample point for ligand free sGC but was less than 200 μW for CO-bound sGC, to avoid accumulation of the CO-photolyzed product. The spinning rate of the sample cell was 3400 rpm, and accumulation times were typically 0.5 h. UV−visible absorption spectra were measured with a

Table 1: Activity of sGC in the Presence of Allosteric Effectors

	specific activity [nmol min^{-1} (mg of protein)$^{-1}$]	relative activity
sGC	70	1
CO−sGC	250	3.5
YC-1−sGC	1100	16
sGC−CO−YC-1	8000	115
NO(SNP)−sGC	9380	134

Hitachi U-3210 spectrophotometer before and after each Raman measurement, and the integrity of each sample was confirmed.

RESULTS

Activity of sGC and Its Stimulation by Allosteric Modulators. SDS−PAGE of this preparation revealed only two bands (α- and β-subunits), and its UV−visible spectrum was a typical ferrous high-spin type, similar to that of a previous preparation (*27*, *36*). The addition of hemin yielded no change in absorption intensity. The activities of sGC and CO and NO adducts in the absence and presence of YC-1 were determined. The results are summarized in Table 1. The basal activity [70 nmol min^{-1} (mg of protein)$^{-1}$] and NO-stimulated activity [9380 nmol min^{-1} (mg of protein)$^{-1}$] of this preparation are similar to those reported by Tomita et al. (*36*). Addition of CO alone stimulated activity by 3.5-fold [250 nmol min^{-1} (mg of protein)$^{-1}$] and YC-1 alone by 16-fold [1100 nmol min^{-1} (mg of protein)$^{-1}$], compared to basal activity. However, the simultaneous presence of CO and YC-1 activated sGC to 115-fold [8000 nmol min^{-1} (mg of protein)$^{-1}$]. Thus, these results confirm synergistic effects reported previously (*19*, *22*, *24*).

The Soret absorption peak of CO−sGC was shifted from 424 to 422 nm following the addition of YC-1. In the presence of GTP, the peak position was shifted to 420 nm (spectra not shown). Denninger et al. (*35*) attributed this to the effect of scattering from the precipitated enzyme upon addition of DMSO-dissolved YC-1. Accordingly, we examined the absorption changes of CO−sGC in the presence of varying final concentrations of DMSO. Addition of DMSO up to 4% (v/v) did not affect the absorption spectrum. On the other hand, the change in YC-1 concentration from 50 to 200 μM (final) did not alter the size of the peak shift (2 nm) from the position in the absence of YC-1. Therefore, the Soret band shift is ascribed solely to interactions between YC-1 and CO−sGC.

Resonance Raman Spectra. RR spectra of CO−sGC excited at 422 nm are shown in Figure 1. In spectrum A, two bands 472 and 488 cm^{-1} exhibited isotopic frequency shifts to 464 and 476 cm^{-1}, respectively, with $^{13}C^{18}O$ as shown in inset A′. Accordingly, both are assigned to the Fe−CO stretching (ν_{Fe-CO}) mode. Tomita and colleagues (*27*) observed a single CO isotope-sensitive band at 472 cm^{-1} (sGC_2). However, in this preparation, two species in the CO-bound state were observed, in agreement with Schelvis et al. (*34*), although it was a single species before CO binding. The extra species gives rise to a minor ν_{Fe-CO} band at 488 cm^{-1} with a frequency close to that reported for sGC_1. When YC-1 was added at a concentration of 120 μM, the intensity of the 472 cm^{-1} band decreased, whereas that of the 488 cm^{-1} band increased, as shown in spectrum B. The addition

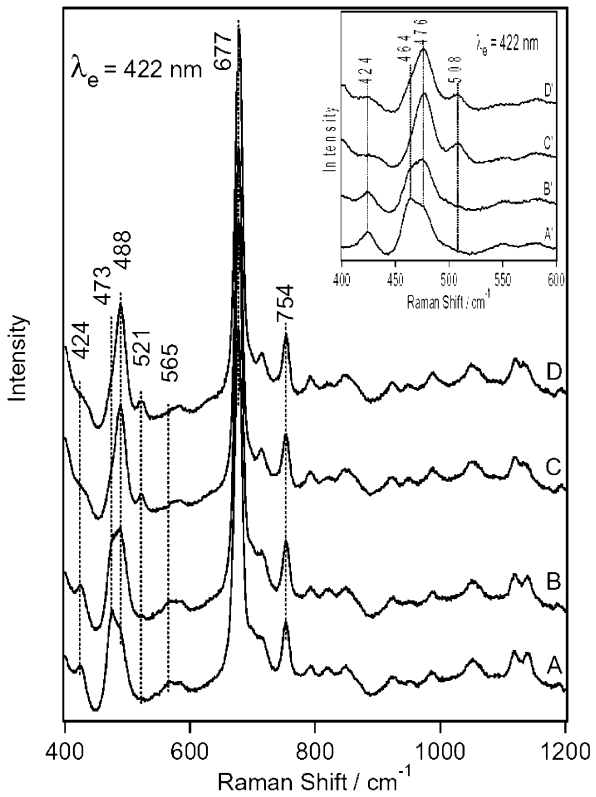

FIGURE 1: Resonance Raman spectra in the 400−1200 cm^{-1} region of CO−sGC (12 μM) in a simple buffer (A) and in the presence of 120 μM YC-1 (B), 120 μM YC-1 and 1 mM GTP (C), and 120 μM YC-1, 1 mM GTP, and 2 mM Mg^{2+} (D). The inset includes the corresponding spectra (A′−D′) of the $^{13}C^{18}O$ adducts. Excitation at 422 nm and 160 μW.

of 1 mM cGMP or GDP to YC-1-bound CO−sGC led to a similar but significantly weaker effect. However, following the addition of GTP to the YC-1-bound CO−sGC at a final concentration of 1 mM, the 472 cm^{-1} band disappeared completely. Instead, a new band appeared at 521 cm^{-1} while the 488 cm^{-1} band further increased in intensity (spectrum C). The Fe−C−O bending mode (δ_{FeCO}) at 565 cm^{-1} in spectrum A lost intensity in spectrum C. Addition of 2 mM $MgCl_2$ to this did not affect the ν_{Fe-CO} frequency, as depicted in spectrum D. When $^{13}C^{18}O$ was used instead of $^{12}C^{16}O$, the 464 and 476 cm^{-1} bands exhibited intensity changes similar to those observed for $^{12}C^{16}O$ (spectra B′ and C′ in the inset representing the addition of YC-1 and GTP, respectively). The new band at 521 cm^{-1} was shifted to 508 cm^{-1}. With regard to the porphyrin modes, the vinyl bending mode at 424 cm^{-1} in spectrum A is replaced by a band at 400 cm^{-1} in spectrum C. The data indicate that the Raman intensities and thus the geometrical structures of two vinyl groups are exchanged between positions 2 and 4 as if the heme were turned over. These results remained unaffected if the order of addition of these compounds was changed (data not shown). Moreover, results were similar in the presence and absence of 20% glycerol in the sGC solution.

To identify the compounds generated by the synergistic effects of YC-1 with GTP, the CO isotope difference spectra were measured with higher resolution. The raw spectra of $^{12}C^{16}O$- and $^{13}C^{18}O$-bound sGC in the presence of YC-1 and GTP were excited at 422 nm, and their differences are depicted in Figure 2. In addition to the 488/476 cm^{-1} pair, other isotope-sensitive bands are clear in the difference

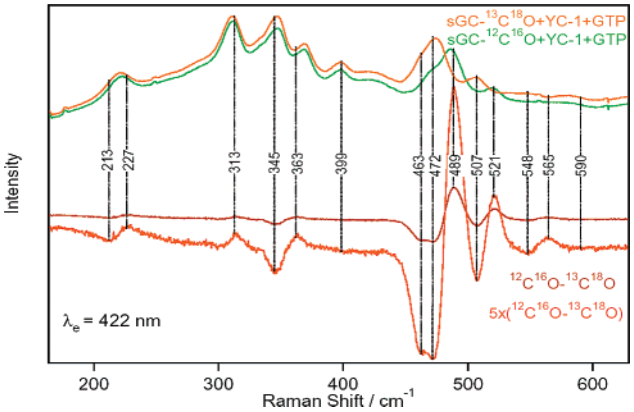

FIGURE 2: CO isotope difference spectrum of CO−sGC in the presence of 120 μM YC-1 and 1 mM GTP. The raw spectra for $^{12}C^{16}O$−sGC and $^{13}C^{18}O$−sGC are represented with green and orange lines, respectively, and their 1:1 difference spectrum is colored brown. Its 5-fold expanded spectrum is colored red. Excitation at 422 nm and 2 mW.

spectrum at 565/548, 521/507, 363/345, and 227/213 cm^{-1} for $^{12}C^{16}O$−sGC/$^{13}C^{18}O$−sGC. The observed peaks at 489/472 and 521/507 cm^{-1} are consistent with the recent results by Makino et al. (*38*). However, in contrast to this report, no isotope-sensitive band was observed at ~590 cm^{-1}. Since the difference peak at 313 cm^{-1} is at the same frequency as that of the raw spectra, this may simply reflect intensity differences. The 521/507 cm^{-1} pair was observed for a model system of a 5c CO heme generated with CO−ferrous porphyrin in CTAB micelles (data not shown), which was shifted to a lower frequency upon binding of 2-methylimidazole to the trans site of CO. Accordingly, this pair should be ascribed to the 5c CO heme of sGC. The assignment of the CO isotope-sensitive bands is discussed later.

Corresponding RR spectra in the high-frequency region are shown in Figure 3. The skeletal vibrations of heme, including ν_2−ν_4 and ν_{10}, are observed at 1562, 1470, 1358, and 1607 cm^{-1}, respectively, for the isolated sGC as shown in spectrum A. The frequencies of these bands indicate that the native sGC contains a 5c-HS ferrous heme in the purified state even in an aerobic environment. There is no trace of a peak around 1500 and 1580 cm^{-1}, where ν_3 and ν_2 bands of the ferrous 6c-LS species are expected. In this regard, this preparation is distinct from that of sGC$_1$ (*25*, *28*).

The ν_2−ν_4 bands of CO−sGC were observed as single bands at 1580, 1497, and 1372 cm^{-1}, respectively, as depicted in spectrum B, indicating the formation of only a ferrous 6c-LS complex. However, in the C−O stretching region of spectrum B, ν_{CO} bands were observed at 1969 (weak) and 1985 cm^{-1}. The difference spectrum with regard to the $^{13}C^{18}O$ adduct is delineated by trace B′ in the inset. The two bands are shifted to 1882 and 1893 cm^{-1}, compatible with the presence of two ν_{Fe-CO} bands. Since the two different conformations of CO−sGC yield no splitting in the vibrations of porphyrin ring, it is likely that the difference between the two conformers is limited to polarity around CO. When the laser power was increased, the observed result was similar to that of spectrum A, indicating photodissociation of CO.

In the presence of 120 μM YC-1, the ν_2 and ν_3 frequencies remained unchanged at 1580 and 1497 cm^{-1}, respectively, as shown in spectrum C. Again, there were two ν_{CO} bands at 1969 and 1985 cm^{-1} (spectrum C′) with relative intensities

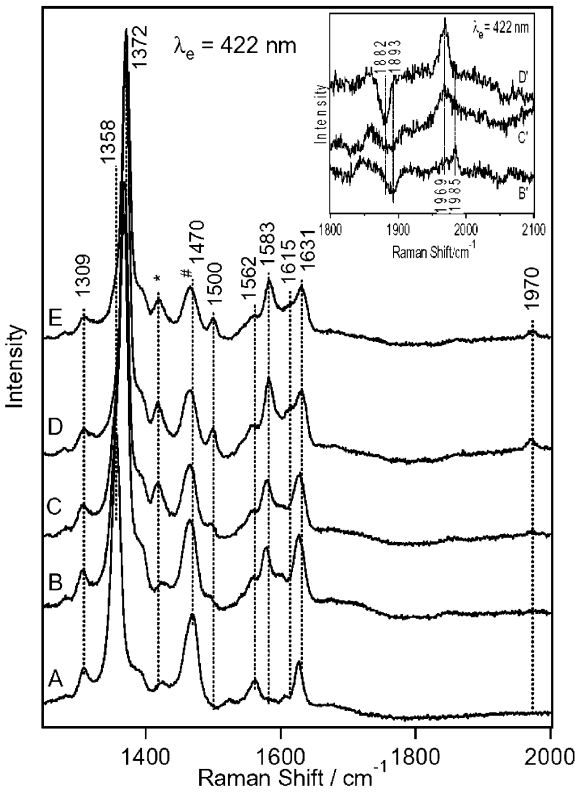

FIGURE 3: Resonance Raman spectra in the 1250−2000 cm^{-1} region of sGC (A) and CO−sGC (12 μM) in a simple buffer (B) or in the presence of 120 μM YC-1 (C), 120 μM YC-1 and 1 mM GTP (D), and 120 μM YC-1, 1 mM GTP, and 2 mM Mg^{2+} (E). Raman bands marked with # and * symbols arise from glycerol and DMSO (YC-1), respectively. The inset depicts the $^{12}C^{16}O$ minus $^{13}C^{18}O$ difference spectra of the corresponding CO adducts (B′−D′). Excitation at 422 nm and 150 μW.

appreciably different from those in spectrum B′. Upon further addition of 1 mM GTP, the ν_2 and ν_3 frequencies hardly changed from those observed with YC-1 alone, but the peaks were more intense. Moreover, the ν_4 band was shifted to a higher frequency by 2 cm^{-1} (spectrum D). In the C−O stretching region, only one ν_{CO} band was observed at 1969 cm^{-1}, with an isotope-shifted band confirmed at 1882 cm^{-1} with $^{13}C^{18}O$, as delineated by spectrum D′ (inset), indicating the presence of a single conformer. Addition of Mg^{2+} to this solution did not alter the spectrum (see spectrum E for details). The synergistic effect of YC-1 and GTP is evident. When the laser power was increased to a level similar to that described above, the spectrum apparently remained unchanged. In particular, the intense ν_4 band appeared at 1372 cm^{-1} but not at 1358 cm^{-1}. This finding indicates that photodissociation hardly takes place or recombination of photodissociated CO is extremely rapid in the presence of YC-1 and GTP, in agreement with reports by Kharitonov et al. (*39*).

Reversibility of YC-1 Binding. To examine whether binding of YC-1 to sGC is reversible, CO−sGC was subjected to gel filtration using a Bio-Rad spin column, and the RR spectra of the treated samples were measured. Spectra A and B in Figure 4 were obtained for the purified enzyme and its CO adduct, respectively, before the treatment. Although the relative intensities of the 473 and 488 cm^{-1} bands are slightly altered in every preparation, the presence of two bands is clear in spectrum A. Upon addition of 120 μM YC-1, the

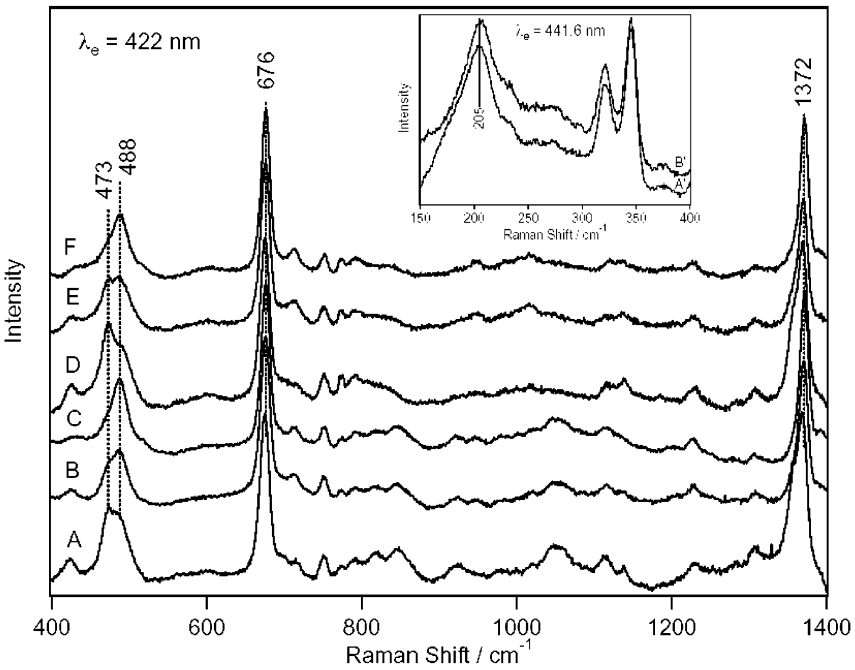

FIGURE 4: RR 422 nm-excited RR spectra for examining the reversibility of YC-1 and GTP binding: (A) starting CO−sGC in a simple buffer, (B) CO−sGC in the presence of 120 μM YC-1, (C) CO−sGC in the presence of 120 μM YC-1 and 1 mM GTP, (D) CO−sGC after gel filtration in a simple buffer, (E) CO−sGC in the presence of 120 μM YC-1, and (F) CO−sGC in the presence of 120 μM YC-1 and 1 mM GTP. The inset shows the 441.6 nm-excited RR spectra of sGC before (A′) and after (B′) gel filtration.

relative intensity of the 473 and 488 cm^{-1} bands was reversed (spectrum B), as expected from Figure 1. In the presence of GTP, the 473 cm^{-1} band disappeared completely (spectrum C). After the measurement of spectrum C, the sample was treated using the Bio-Rad spin column. The eluted enzyme exhibited an RR spectrum of reduced sGC without CO (spectrum not shown). A 441.6 nm excitation of the enzyme led to a ν_{Fe-His} band at 205 cm^{-1} (spectrum B′ in the inset), similar to that observed before treatment (trace A′ in the inset). Addition of CO yielded spectrum D, in which the 488 cm^{-1} band decreased in intensity, similar to the starting sample. Addition of YC-1 to the gel-filtered sample increased the intensity of the 488 cm^{-1} band, as shown in spectrum E. Further treatment with GTP resulted in a single band at 488 cm^{-1}, as depicted in spectrum F. Thus, the reproducibility of the whole phenomenon was confirmed, demonstrating reversible binding of YC-1 and GTP to sGC. However, it must be noted that this conclusion is limited to YC-1 and GTP, which affect the Fe−CO moiety.

Figure 5 summarizes the effects of substrate analogues on RR spectra in the low-frequency region. The excitation wavelength is shifted to 413.1 nm to enhance the Raman intensity of the new species. Spectra A and B depict CO−sGC in the absence and presence of YC-1, respectively. The 489 cm^{-1} band is very weak in the absence of YC-1 (A) but gains intensity upon addition of YC-1 (B). Spectra C and D were obtained following the addition of GDP and cGMP, respectively, to the solution of B. The relative intensities of the 489 and 473 cm^{-1} bands remain unaltered, and the 522 cm^{-1} band exhibits a relative intensity similar to that in spectrum B. The δ_{FeCO} band at 565 cm^{-1} is recognizable in spectrum A, but hardly evident in spectra B−D, indicating that the band belongs to the 473 cm^{-1} species. On the other hand, when a substrate analogue, GTP-γ-S, was added to the solution of spectrum B, the relative intensities of the 489

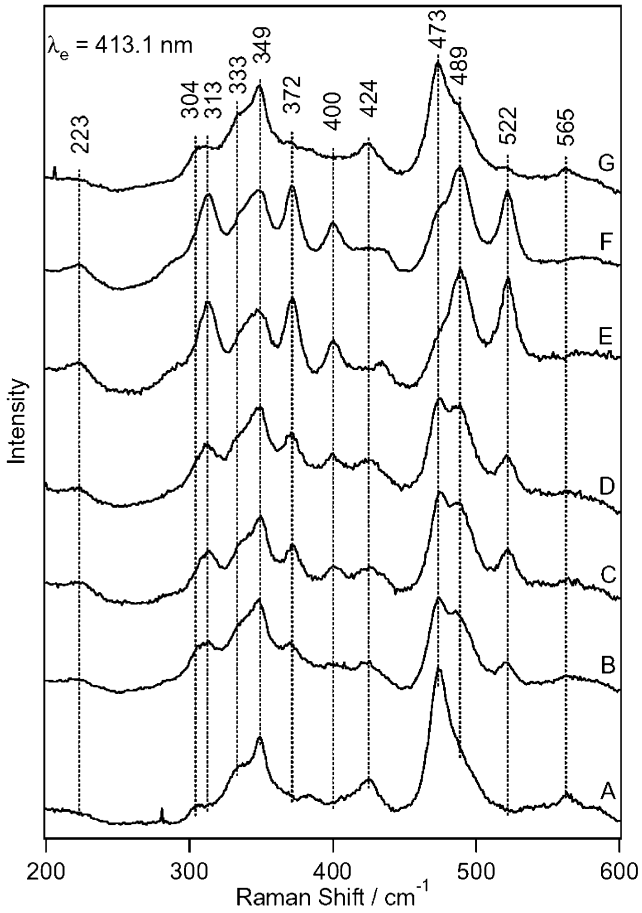

FIGURE 5: RR spectra of bovine CO−sGC upon addition of substrate analogues (A) in the absence of any added compounds and (B) in the presence of 120 μM YC-1, (C) 120 μM YC-1 and GDP, (D) 120 μM YC-1 and cGMP, (E) 120 μM YC-1 and GTP-γ-S, (F) 120 μM YC-1 and GTP, and (G) 120 μM YC-1 and ATP.

and 473 cm^{-1} bands were significantly altered, and the 522 cm^{-1} band was intensified (spectrum E). These results are similar to those obtained for GTP, which is shown in spectrum F for comparison. The intensity of the vinyl bending mode at 424 cm^{-1}, which is clear in spectrum A, is reduced upon binding of YC-1 and GTP, and new bands are observed at 400, 313, and 223 cm^{-1}. No peak is evident around 550−600 cm^{-1}, despite measurement conditions under which the excitation wavelength is more favorable to the YC-1- and GTP-bound forms. Unexpectedly, when ATP was added to the YC-1-bound form, the relative intensities of the 489 and 473 cm^{-1} bands were similar to those observed in the absence of YC-1 and GTP, and the bands at 522, 400, 313, and 223 cm^{-1} were significantly reduced in intensity (spectrum G). Therefore, it is evident that ATP inhibits the effects of YC-1 and GTP.

DISCUSSION

Effects of Allosteric Modulators. While Fan et al. (*25*) identified two ν_3 bands at 1470 (5c-HS) and 1493 cm^{-1} (6c-LS), for the heme-reconstituted protein, Deinum et al. (*26*) and Tomita et al. (*27*) reported a single ν_3 band at 1473 cm^{-1} for the native sGC purified as the heme-containing form (Figure 3). Consistent with the latter observation, sGC purified from bovine lung in our study gave rise to a single ν_3 band in the ferrous 5c-HS region, and yielded a single Fe−His stretching Raman band at 204 cm^{-1}, indicating the presence of a single form. The latter band is present for only the ferrous 5c-HS heme. However, its CO-bound form yielded two species. Schelvis et al. (*34*) detected the two corresponding ν_{Fe-CO} bands for recombinant rat lung $\beta1$(1−385) protein expressed in *E. coli*, namely, intense and weak bands at 478 and 495 cm^{-1}, respectively. These authors re-examined their early data (*26*) of bovine lung sGC, and confirmed the presence of a minor component (*34*). Thus, the findings presented here are compatible with the previous reports.

On one hand, the population of the minor component in the ν_{Fe-CO} band intensity increased upon addition of YC-1, which is similar to the observation of Denninger et al. (*35*), and on the other, the coexistence of YC-1 and CO in the sGC solution induced a synergistic effect on reactivity at the catalytic site. This population change was significantly promoted in the presence of GTP. Imidazole has a similar synergistic effect on activity and the ν_{Fe-CO} band (*40*). The GTP effect was previously reported with an NO adduct of sGC (*27*). However, in our experiments, no effects were observed when GTP was added to CO−sGC without YC-1. The YC-1 effect on the ν_{Fe-CO} band is also observed for heme domain protein β_1(1−385) (*34*).

Selecting the spectrum observed in the presence of both YC-1 and GTP as a spectrum of allosterically activated CO−sGC appears to be informative. The coexistence of YC-1 and GTP in the purified enzyme without CO did not alter the Fe−His stretching frequency and other parts of the RR spectra. Therefore, the synergistic effect would arise from the distal side of heme and be specific for CO−sGC. Since the frequencies of the main ν_{Fe-CO} bands in the presence and absence of allosteric effectors are close to those of CO−sGC_1 and CO−sGC_2, respectively, this discussion focuses on the structural differences between these two species.

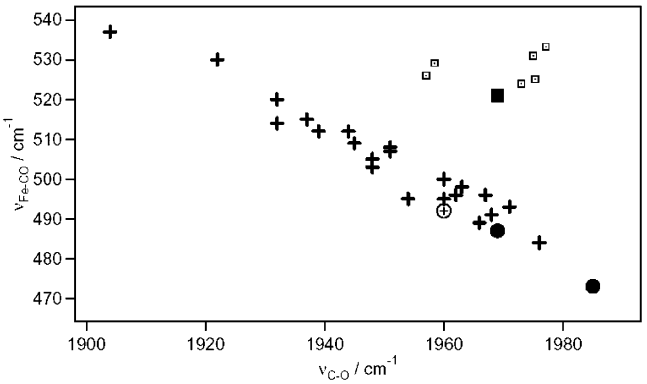

FIGURE 6: The ν_{FeCO} vs ν_{CO} plot. The values from the present study are plotted as CO-sGC_1 and CO-sGC_2 (●). Markers, + and ⊡, denote the His-ligated 6c and 5c proteins, respectively. Marker (●) represents CO-sGC with or without YC-1 and GTP, whereas (⊕) denotes CO-sGC in the presence of imidazole. Marker (■) represents 5c CO-sGC (with YC-1 and GTP).

However, it is emphasized that the simple CO−sGC without effectors contains two forms with ν_{Fe-CO} bands identified at 473 (main) and 488 (minor) cm^{-1}, while allosterically activated CO−sGC also contains two forms, with ν_{Fe-CO} bands at 488 and 521 cm^{-1}.

Assignments of CO Isotope-Sensitive Bands. Figures 1 and 2 demonstrate that one of two forms of simple CO−sGC gives rise to ν_{Fe-CO} at 473 cm^{-1} and ν_{CO} at 1985 cm^{-1}, while the other produces ν_{Fe-CO} at 488 cm^{-1} and ν_{CO} at 1969 cm^{-1}. In a plot of ν_{Fe-CO} versus ν_{CO}, both fall on the same straight line for histidine-coordinated heme proteins, as illustrated in Figure 6. Accordingly, both forms adopt the 6c-LS form with histidine as a trans ligand of CO. The higher ν_{Fe-CO} and lower ν_{CO} frequencies reflect a more polar environment around CO with His as the trans ligand (*32*, *33*). Therefore, the presence of YC-1 and GTP makes the heme pocket slightly more polar than that in its absence. The 473 cm^{-1} species yields a δ_{FeCO} Raman band at 565 cm^{-1}. As the δ_{FeCO} Raman intensity is stronger for a distorted structure than for a linear one (*41*), the 473 cm^{-1} form may have a distorted Fe−C−O geometry. All the porphyrin modes exhibited no splitting. Accordingly, the differences between the absence and presence of allosteric modulators must be attributed solely to structural variations in the heme distal side.

Figure 7 illustrates the mass dependences of the CO isotope-sensitive bands. The 473 (B) and 565 cm^{-1} (E) pair arising from simple CO−sGC exhibits typical monotonic and zigzag patterns, indicating ordinary Fe−C−O geometry of CO−heme proteins. On the other hand, the 488 (C) and 521 cm^{-1} (D) bands also exhibit a monotonic dependence, suggesting that both arise from the Fe−CO stretching modes with nearly linear Fe−CO geometry. If the Fe−C−O geometry is bent, the bending and stretching modes are severely mixed with each other, and the resultant two modes are expected to exhibit the mixed isotope shift pattern. In particular, the ^{13}C isotope shift of ν_{Fe-CO} becomes larger for a more bent geometry (*42*). The frequency difference between the 488 and 521 cm^{-1} bands is attributed to the presence and absence of the trans ligand of CO, and is satisfactorily interpreted in terms of the antibonding contribution from the d_{z^2} orbital to the Fe−CO σ bonding for the 6c species (*33*). The 224 cm^{-1} band has a slight zigzag character, suggesting the appearance of a tilting vibration

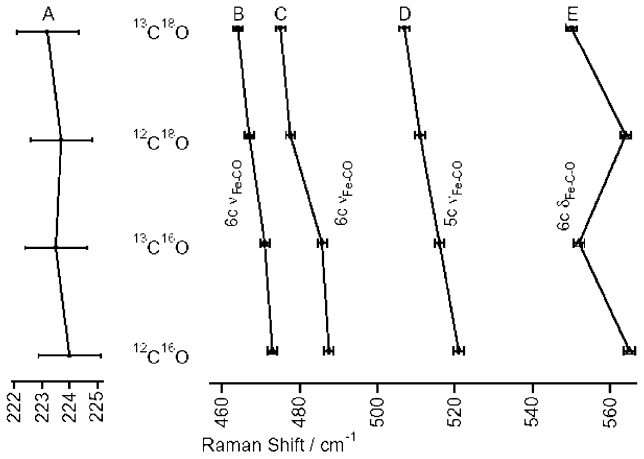

FIGURE 7: Mass dependence of the CO isotope-sensitive bands observed for sGC. Traces A, C, and D represent the results observed for CO−sGC in the presence of YC-1 and GTP, whereas traces B and E show the results from the simple CO−sGC.

of the Fe−CO bond of the 5c heme. These results suggest that the CO adducts that are present are unlikely to assume a significantly distorted geometry.

In Figure 2, an additional CO isotope-sensitive band is evident at around 360 cm^{-1}. These bands are reported for several heme proteins (*43*), and were once assigned to the Fe−C−O bending fundamental (*44*). Isotope sensitivity was confirmed by Kincaid and co-workers, but the bands were reassigned to a heme vibration coupled with the CO bending mode (*45*).

Binding Model of YC-1. Stasch et al. (*46*) observed that an NO-independent activator of sGC, a derivative of BAY 41-2272, is covalently bound to Cys238 and Cys243 of the α-subunit, and that binding of BAY 41-2272 is inhibited when YC-1 is already bound to sGC. On the basis of these data, they suggested the possibility of YC-1 binding to these residues. However, our study demonstrates that binding of YC-1 is reversible, and the covalent binding scheme is not applicable to YC-1. Another NO- and heme-independent activator, BAY 58-2667, binds to the heme-binding site, and interacts with β1 Tyr135 and Arg139 (*47*). On the other hand, mutation of α1 Cys596 to Ser leads to a marked increase in nonstimulated activity and a decreased level of stimulation by YC-1 or NO (*48*). More recent mutation experiments indicate that Cys594 is a key for YC-1 response (*49*). Although we confirm the binding of YC-1 to the heme pocket, it is possible that another YC-1 molecule binds to these residues but has little effect on the heme moiety.

Since YC-1 contains an N atom which may bind to the heme iron, we hypothesize that one CO adduct contains the N atom of YC-1 as its trans ligand. One hypothesis is that YC-1 occupies the distal side, while CO binds the proximal side instead of His105. The idea that this species yields a ν_{Fe-CO} of 488 cm^{-1} is compatible with the idea that NO can bind both sides of heme (*50*). In this case, the CO-photodissociated transient species is expected to provide the Fe−N stretching mode at a frequency different from that of the Fe−His stretching mode. In practice, however, the photodissociated transient species observed for CO−sGC in the presence of YC-1 and GTP with high laser power yielded only the 204 cm^{-1} band in the vicinity of 200 cm^{-1}. Therefore, there is no experimental basis for postulating that YC-1 is coordinated to heme. It is most likely, from the absence of multiplicity in the marker bands of heme of CO−sGC in the presence of YC-1 and GTP, that the heme distal pocket is perturbed by the allosteric modulators.

These Raman data strongly suggest that YC-1 binds to the distal side of the heme pocket with a geometry in which its HO group directs the heme-bound CO and its aromatic ring to the heme vinyl groups to alter the vinyl vibrations. The location of YC-1 in this geometry may block the protein pathway of CO to solution and produce a more polar environment around the bound CO, compatible with changes in ν_{Fe-CO} and ν_{CO} frequencies upon YC-1 binding. The binding of a bulky group near the heme causes a protein conformational change, leading to a structural alteration at a distant substrate-binding site. The concerted effect of YC-1 and GTP indicates that the structural changes by YC-1 and GTP are along the identical direction, but opposite to those by ATP. If this is the case, rapid recombination of photodissociated CO to heme in the presence of YC-1 is understandable, since an exit of CO from the heme pocket is closed. Since YC-1 does not interact directly with heme, neither the Fe−His stretching mode nor the visible absorption spectrum of the reduced heme is influenced by binding of YC-1. This interpretation does not rule out the binding of another YC-1 to the α−subunit. Since the binding effect of YC-1 and GTP appears in the Fe−C−O moiety of the β-subunit, but not in the Fe−His moiety of the photodissociated transient state, it is difficult to believe that a large-scale conformational change propagated from the α- to β-subunit for binding of YC-1 and GTP. Although activation by NO is accompanied by the rupture of the Fe−His bond, the common features in the two activation processes by NO, and by CO and YC-1, remain to be clarified.

REFERENCES

1. Schmidt, H. H., Lohmann, S. M., and Walter, U. (1993) The nitric oxide and cGMP signal transduction system: regulation and mechanism of action, *Biochim. Biophys. Acta 1178*, 153−175.
2. Hobbs, A., and Ignarro, L. J. (1996) Nitric oxide-cyclic GMP signal transduction system, *Methods. Enzymol. 269*, 134−148.
3. Garbers, D. L., Koesling, D., and Schultz, G. (1994) Guanylyl cyclase receptors, *Mol. Biol. Cell 5*, 1−5.
4. Kamisaki, Y., Saheki, S., Nakane, M., Palmieri, J. A., Kuno, T., Chang, B. Y., Waldman, S. A., and Murad, F. (1986) Soluble guanylate cyclase from rat lung exists as a heterodimer, *J. Biol. Chem. 261*, 7236−7241.
5. Mulsch, A., and Gerzer, R. (1991) Purification of heme-containing soluble guanylyl cyclase, *Methods Enzymol. 195*, 377−383.
6. Stone, J. R., and Marletta, M. A. (1994) Soluble guanylate cyclase from bovine lung: activation with nitric oxide and carbon monoxide and spectral characterization of the ferrous and ferric states, *Biochemistry 33*, 5636−5640.
7. Harteneck, C., Koesling, D., Soling, A., Schultz, G., and Bohme, E. (1990) Expression of soluble guanylyl cyclase. Catalytic activity requires two enzyme subunits, *FEBS Lett 272*, 221−223.
8. Buechler, W. A., Nakane, M., and Murad, F. (1991) Expression of soluble guanylate cyclase activity requires both enzyme subunits, *Biochem. Biophys. Res. Commun. 174*, 351−357.
9. Zhao, Y., and Marletta, M. A. (1997) Localization of the heme binding region in soluble guanylate cyclase, *Biochemistry 36*, 15959−15964.
10. Friebe, A., Wedel, B., Harteneck, C., Foerster, J., Schultz, G., and Koesling, D. (1997) Functions of conserved cysteines of soluble guanylyl cyclase, *Biochemistry 36*, 1194−1198.
11. Zhao, Y., Schelvis, J. P. M., Babcock, G. T., and Marletta, M. A. (1998) Identification of histidine 105 in the β1 subunit of soluble guanylate cyclase as the heme proximal ligand, *Biochemistry 37*, 4502−4509.

12. Ignarro, L. J., and Kadowitz, P. J. (1985) The pharmacological and physiological role of cyclic GMP in vascular smooth muscle relaxation, *Annu. Rev. Pharmacol. Toxicol. 25*, 171−191.
13. Azuma, H., Ishikawa, M., and Sekizaki, S. (1986) Endothelium-dependent inhibition of platelet aggregation, *Br. J. Pharmacol. 88*, 411−415.
14. Garthwaite, J., Charles, S. L., and Chess-Williams, R. (1988) Endothelium-derived relaxing factor release on activation of NMDA receptors suggests role as intercellular messenger in the brain, *Nature 336*, 385−388.
15. Burstyn, J. N., Yu, A. E., Dierks, E. A., Hawkins, B. K., and Dawson, J. H. (1995) Studies of the heme coordination and ligand binding properties of soluble guanylyl cyclase (sGC): characterization of Fe(II)sGC and Fe(II)sGC(CO) by electronic absorption and magnetic circular dichroism spectroscopies and failure of CO to activate the enzyme, *Biochemistry 34*, 5896−5903.
16. Stone, J. R., and Marletta, M. A. (1995) Heme stoichiometry of heterodimeric soluble guanylate cyclase, *Biochemistry 34*, 14668−14674.
17. Karlsson, J. O., Axelsson, K. L., and Andersson, R. C. (1985) Effects of hydroxyl radical scavengers KCN and CO on ultraviolet light-induced activation of crude soluble guanylate cyclase, *J. Cyclic Nucleotide Protein Phosphorylation Res. 10*, 309−315.
18. Brune, B., and Ullrich, V. (1987) Inhibition of platelet aggregation by carbon monoxide is mediated by activation of guanylate cyclase, *Mol. Pharmacol. 32*, 497−504.
19. Friebe, A., Schultz, G., and Koesling, D. (1996) Sensitizing soluble guanylyl cyclase to become a highly CO-sensitive enzyme, *EMBO J. 15*, 6863−6868.
20. Wu, C. C., Ko, F. N., Kuo, S., Lee, F. Y., and Teng, C. M. (1995) YC-1 inhibited human platelet aggregation through NO-independent activation of soluble guanylate cyclase, *Br. J. Pharmacol. 116*, 1973−1978.
21. Wu, C. C., Ko, F. N., and Teng, C. M. (1997) Inhibition of platelet adhesion to collagen by cGMP-elevating agents, *Biochem. Biophys. Res. Commun. 231*, 412−416.
22. Mulach, A., Bauersachs, J., Schafer, A., Stasch, J. P., Kast, R., and Buss, E. R. (1997) Effect of YC-1, an NO-independent, superoxide-sensitive stimulator of soluble guanylyl cyclase, on smooth muscle responsiveness to nitrovasodilators, *Br. J. Pharmacol. 120*, 681−689.
23. Galle, J., Zabel, U., Hubner, U., Hatzelmann, A., Wagner, B., Wanner, C., and Schmide, H. H. H. (1999) Effects of the soluble guanylyl cyclase activator, YC-1, on vascular tone, cyclic GMP levels and phosphodiesterase activity, *Br. J. Pharmacol. 127*, 195−203.
24. Stone, J. R., and Marletta, M. A. (1998) Synergistic activation of soluble guanylate cyclase by YC-1 and carbon monoxide: implications for the role of cleavage of the iron-histidine bond during activation by nitric oxide, *Chem. Biol. 5*, 255−261.
25. Fan, B. C., Gupta, G., Danziger, R. S., Friedman, J., and Rousseau, D. L. (1998) Resonance Raman characterization of soluble guanylate cyclase expressed from baculovirus, *Biochemistry 37*, 1178−1184.
26. Deinum, G., Stone, J. R., Babcock, G. T., and Marletta, M. A. (1996) Binding of nitric oxide and carbon monoxide to soluble guanylate cyclase as observed with Resonance Raman spectroscopy, *Biochemistry 35*, 1540−1547.
27. Tomita, T., Ogura, T., Tsuyama, S., Imai, Y., and Kitagawa, T. (1997) Effects of GTP on bound nitric oxide of soluble guanylate cyclase probed by resonance Raman spectroscopy, *Biochemistry 36*, 10155−10160.
28. Yu, A. E., Hu, S. Z., Spiro, T. G., and Burstyn, J. N. (1994) Resonance Raman Spectroscopy of Soluble Guanylyl Cyclase Reveals Displacement of Distal and Proximal Heme Ligands by NO, *J. Am. Chem. Soc. 116*, 4117−4118.
29. Stone, J. R., Sandos, R. H., Dunham, W. R., and Marletta, M. A. (1995) Electron paramagnetic resonance spectral evidence for the formation of a pentacoordinate-nitrosyl-heme complex on soluble guanylate cyclase, *Biochem. Biophys. Res. Commun. 207*, 572−577.
30. Gerzer, R., Bohme, E., Hofmann, F., and Schultz, G. (1981) Soluble guanylate cyclase purified from bovine lung contains heme and copper, *FEBS Lett. 132*, 71−74.
31. Vogel, K. M., Hu, S. Z., Spiro, T. G., Dierks, E. A., Yu, A. E., and Burstyn, J. N. (1999) Variable forms of soluble guanylyl cyclase: protein−ligand interactions and the issue of activation by carbon monoxide, *J. Biol. Inorg. Chem. 4*, 804−813.
32. Phillips, G. N., Jr., Teodoro, M. L., Li, T., Smith, B., and Olson, J. S. (1999) Bound CO Is a Molecular Probe of Electrostatic Potential in the Distal Pocket of Myoglobin, *J. Phys. Chem. B 103*, 8817−8829.
33. Vogel, K. M., Kozolowski, P. M., Zgierski, M. Z., and Spiro, T. G. (1999) Determinants of the FeXO [X = C, N, O] Vibrational Frequencies in Heme Proteins and Models from Experiment and Density Functional Theory, *J. Am. Chem. Soc. 121*, 9915−9921.
34. Schelvis, J. P. M., Zhao, Y., Marletta, M. A., and Babcock, G. T. (1998) Resonance Raman characterization of the heme domain of soluble guanylate cyclase, *Biochemistry 37*, 16289−16297.
35. Denninger, J. W., Schelvis, J. P. M., Brandish, P. E., Zhao, Y., Babcock, G. T., and Marletta, M. A. (2000) Interaction of soluble guanylate cyclase with YC-1: kinetic and resonance Raman studies, *Biochemistry 39*, 4191−4198.
36. Tomita, T., Tsuyama, S., Imai, Y., and Kitagawa, T. (1997) Purification of bovine soluble guanylate cyclase and ADP-ribosylation on its small subunit by bacterial toxins, *J. Biochem. 122*, 531−536.
37. Bradford, M. M. (1976) A rapid and sensitive method for the quantitation of microgram quantities of protein utilizing the principle of protein-dye binding, *Anal. Biochem. 72*, 248−254.
38. Makino, R., Obayashi, E., Homma, N., Shiro, Y., and Hori, H. (2003) YC-1 facilitates release of the proximal His residue in the NO and CO complexes of soluble guanylate cyclase, *J. Biol. Chem. 278*, 11130−11137.
39. Kharitonov, V. G., Sharma, V. S., Magde, D., and Koesling, D. (1999) Kinetics and equilibria of soluble guanylate cyclase ligation by CO: effect of YC-1, *Biochemistry 38*, 10699−10706.
40. Pal, B., Li, Z., Ohta, T., Takenaka, S., Tsuyama, S., and Kitagawa, T. (2004) Resonance Raman study on synergistic activation of soluble guanylate cyclase by imidazole, YC-1 and GTP, *J. Inorg. Biochem. 98*, 824−832.
41. Yu, N. T., Kerr, E. A., Ward, B., and Chang, C. K. (1983) Resonance Raman detection of Fe−CO stretching and Fe−C−O bending vibrations in sterically hindered carbonmonoxy "strapped hemes". A structural probe of Fe−C−O distortion, *Biochemistry 22*, 4534−4540.
42. Nagai, M., Yoneyama, Y., and Kitagawa, T. (1991) Unusual CO bonding geometry in abnormal subunits of hemoglobin M Boston and hemoglobin M Saskatoon, *Biochemistry 30*, 6495−6503.
43. Hirota, S., Ogura, T., Shinzawa-Itoh, K., Yoshikawa, S., Nagai, M., and Kitagawa, T. (1994) Vibrational Assignments of the FeCO Unit of CO-Bound Heme Proteins Revisited: Observation of a New CO-Isotope-Sensitive Raman Band Assignable to the FeCO Bending Fundamental, *J. Phys. Chem. 98*, 6652−6660.
44. Hirota, S., Ogura, T., and Kitagawa, T. (1995) Observation of Nonfundamental Fe−O_2 and Fe−CO Vibrations and Potentioal Anharmonicities for Oxyhemoglobin and Carbon monoxyhemoglobin. Evidences Supporting a New Assignment of the Fe−C−O Bending Fundamental, *J. Am. Chem. Soc. 117*, 821−822.
45. Rajani, C., and Kincaid, J. R. (1998) Resonance Raman Studies of Hemoglobin with Selectively Deuterated Hemes. A New Perspective on the Controversial Assignment of the references. Fe−CO Bending Mode, *J. Am. Chem. Soc. 120*, 7278−7285.
46. Stasch, J.-P., Becker, E. M., Alonso-Alija, C., Apeler, H., Dembowsky, K., Feurer, A., Gerzer, R., Minuth, T., Perzborn, E., Pleiss, U., Schroder, H., Schroeder, W., Stahl, E., Steinke, W., Straub, A., and Schramm, M. (2001) NO-independent regulatory site on soluble guanylate cyclase, *Nature 410*, 212−215.
47. Schmidt, P. M., Schramm, M., Schroder, H., Wunder, F., and Stasch, J.-P. (2004) Identification of residues crucially involved in the binding of the heme moiety of soluble guanylate cyclase, *J. Biol. Chem. 279*, 3025−3032.
48. Friebe, A., Russwurm, M., Mergia, E., and Koesling, D. (1999) A point-mutated guanylyl cyclase with features of the YC-1-stimulated enzyme: implications for the YC-1 binding site? *Biochemistry 38*, 15253−15257.
49. Lamothe, M., Chang, F.-J., Balashova, N., Shirokov, R., and Beuve, A. (2004) Functional Characterization of Nitric Oxide and YC-1 Activation of Soluble Guanylyl Cyclase: Structural Implication for the YC-1 Binding Site? *Biochemistry 43*, 3039−3048.
50. Andrew, C. R., George, S. J., Lawson, D. M., and Eady, R. R. (2002) Six- to five-coordinate heme-nitrosyl conversion in cytochrome *c′* and its relevance to guanylate cyclase, *Biochemistry 41*, 2353−2360.

BI0489208